Asociación Argentina
de Mecánica Computacional

Mecánica Computacional Vol XXXI, págs. 3811-3826 (artículo completo)
Alberto Cardona, Paul H. Kohan, Ricardo D. Quinteros, Mario A. Storti (Eds.)
Salta, Argentina, 13-16 Noviembre 2012

NUMERICAL MODELLING OF A CERVICAL SPINE DISCECTOMY

Ester Comellas[a], Sergio Oller[a], Jose M. Poblete[b], Joan Berenguer[c] and Alberto Prats-Galino[d]

[a] *CIMNE. International Center for Numerical Methods in Engineering. UPC. Technical University of Catalonia (Barcelona Tech). Edif. C1, Campus Nord, c/ Jordi Girona 1-3, 08034 Barcelona, Spain. ecomellas@cimne.upc.edu, http://www.upc.edu, http://www.cimne.com*

[b] *Department of Neurosurgery, Hospital Clinic, Faculty of Medicine, Universitat de Barcelona, c/ Villarroel 170, 08036 Barcelona, Spain. http://www.hospitalclinic.org/, http://www.ub.edu*

[c] *Department of Radiology, Neuroradiology Division, Hospital Clinic, Faculty of Medicine, Universitat de Barcelona, c/ Villarroel 170, 08036 Barcelona, Spain. jberen@clinic.ub.es, http://www.hospitalclinic.org/*

[d] *Laboratory of Surgical NeuroAnatomy, Faculty of Medicine, Universitat de Barcelona, c/ Casanova 143, 08036 Barcelona, Spain. aprats@ub.edu, http://www.ub.edu*

Keywords: Finite Element Analysis (FEA), Constitutive Modelling, Cervical Spine, Anterior Cervical Discectomy (ACD).

Abstract. Cervical spine discectomy is a relatively common medical procedure which entails the surgical removal of a herniated intervertebral disc which is then replaced with an adequate prosthesis. Surgeons rely on their expertise to minimize the damage induced on the adjacent vertebrae and discs during this invasive procedure in order to reduce the patient's postsurgical distress. A typical cervical spine discectomy has been modelled and tested using the Finite Element Method (FEM) with the intention of contributing to better elucidate its immediate physical consequences on the vertebrae and intervertebral discs. Internal stresses, strains and damage levels can be obtained through the use of FE models, which can prove useful in improving surgical procedures or tailoring them to the need of particular patients. To this aim, a model of four cervical vertebrae with their corresponding discs has been built. Spinal ligaments, zygapophyseal joints and uncovertebral joints have also been included. The vertebrae have been modelled using a damage model whilst the intervertebral discs and ligaments have been treated as separate hyperelastic materials. Also, the nucleus and the annulus of the discs have been differentiated. The problem has been solved following non-linear large deformation theory and considering prestress in the ligaments. The model's accuracy has been assessed through comparison of previously published results for different spinal movements (N. Kallemeyn et al., *Med Eng Phys*, 32(5):482-489 (2010)). Then, the model has been numerically tested for a load case representative of the discectomy procedure.

1 INTRODUCTION

Anterior cervical discectomy (ACD) is a common medical procedure used to treat cervical spine conditions such as degenerative disc disease or a herniated disc (Donaldson and Nelson (2002)). It consists in surgically removing the affected intervertebral disc and replacing it with an adequate prosthesis. The affected disc is accessed via the anterior part of the spine through a small incision performed near the front of the neck. Soft tissues are separated in order to reach the spine and, then, the vertebrae adjacent to the diseased disc are forced apart a few millimeters with the aid of adequate surgical tools. Surgeons are concerned that this displacement forced upon the vertebrae induces considerable stress upon the adjacent discs and vertebrae, directly relating to the patient's postsurgical distress. At present, surgeons rely solely on their expertise to minimize the damage induced by this action as they do not have the means to know how the components of the cervical spine will internally respond to the external stimuli. Finite element modelling offers an insight into understanding the internal mechanical response of the spine to induced loads, which may lead to improved techniques during the procedure.

There is a significant amount of Finite Element Analysis (FEA) studies on models of the cervical spine available in literature with varying degrees of detail and completeness in the anatomic and constitutive modelling according to the goal of each study. See, for example: del Palomar et al. (2008); DeWit (2012); Hussain et al. (2012); Kallemeyn et al. (2010); Li (2010); Li and Lewis (2010); Tchako (2009); Teo and Ng (2001); Zhang (2011); Zhang et al. (2005, 2006). However, the authors have found none where the inmediate effects during a discectomy operation on the internal structure of the spine are analyzed. The goal of this study was to construct an anatomically accurate Finite Element (FE) model of the cervical spine comprising the C3-C6 vertebrae (Fig. 1) and subject it to a typical ACD procedure with the ultimate aim of better understanding the internal biomechanical behaviour of the spine during the surgical operation. The model developed has been previously compared to published results in order to assess its accuracy.

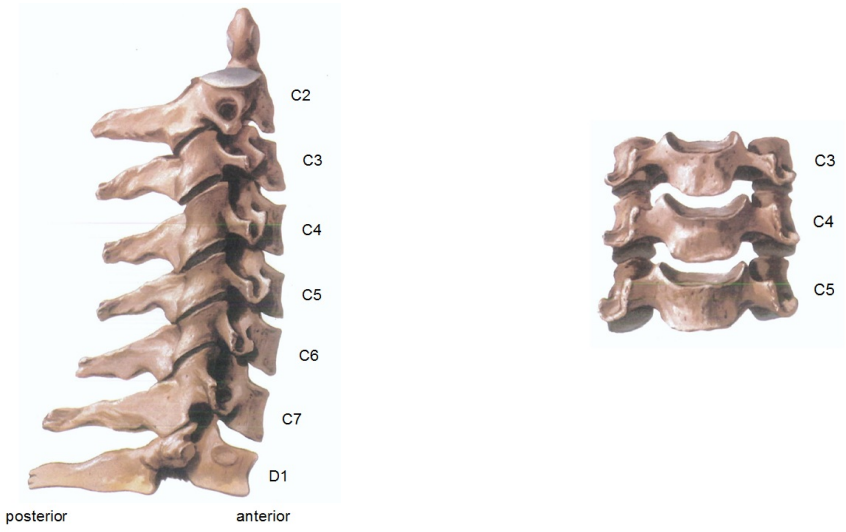

Figure 1: Lateral view of the cervical spine (left) and anterior view of the C3-C5 vertebrae (right), adapted from Netter (1999).

2 MATERIALS AND METHODS

A three-dimensional FE model of four adjacent cervical vertebrae (C3-C6) has been developed with the aim of numerically modeling the discectomy of the C4-C5 disc. The model comprises the vertebral bodies, the intervertebral discs, the uncovertebral and zygapophyseal joints and the main ligaments that participate in the stabilization of the middle cervical spine. The geometry of the C3 and C4 vertebrae was obtained using digitalized quantitative axial computed tomography (CT) scans of an adult cadaveric specimen. The boundary of the corresponding intervertebral disc was approximated using MR scans. Then, due to lack of CT scans of the C5 and C6 vertebrae, these and their corresponding discs were generated by copying the C4 vertebra and the C3-C4 disc. All the ligaments in the model where created from scratch with the aid of the GiD® preprocessor for numerical simulations following professional medical directions. The FE program PLCd, developed by the RMEE Dept. of the UPC, was used to perform the non-lineal analyses.

2.1 Finite Element Model

All the components of the model were meshed using quadratic tetrahedral elements (Fig. 2). Vertebras were divided into the body and the posterior parts, being the body further divided into a cortical shell which encases a trabecular core. In the intervertebral discs, annulus and nucleus were distinguised (Fig. 3). The modelled ligaments include: the posterior longitudinal ligament (PLL), the ligamentum flavum (LF) and the interspinous ligament (IL) (Fig. 4). The anterior longitudinal ligament has not been included as this ligament is cut by the neurosurgeon in the ACD procedure. The contribution of the other ligaments has not been considered as significant in the loading induced by the ACD. The vertebrae were modelled using an isotropic scalar damage material model whislt both, discs and ligaments, were assigned an isotropic neo-Hookean hyperelastic constitutive model. Finally, the uncovertebral and zygapophyseal joints were also modelled with tetrahedral elements but given a substantially higher rigidity to simulate the behaviour of these joints in the cervical spine.

The mechanical properties used in the model are those reported in literature as common to the cervical spine (del Palomar et al. (2008); Kallemeyn et al. (2010); Kumaresan et al. (1999); Li and Lewis (2010)) and are shown in Table 1. The damage properties of the different bone tissues were chosen to approximately match the data in Fig. 5.

2.2 Constitutive Models

2.2.1 Hyperelasticity

Hyperelasticity or Green elasticity is used to model materials which respond elastically when subjected to large deformations. The Clausius-Duhem inequality must be fullfilled at all times for the model to be thermodynamically admissible. Considering solely purely deformative processes where there does not intervene any changes in entropy or temperature and taking into account that hyperelastic materials have null internal dissipation due to the reversible character of their loading processes, this inequality is reduced to

$$\dot{\Psi} = \mathbf{S} : \dot{\mathbf{E}} \tag{1}$$

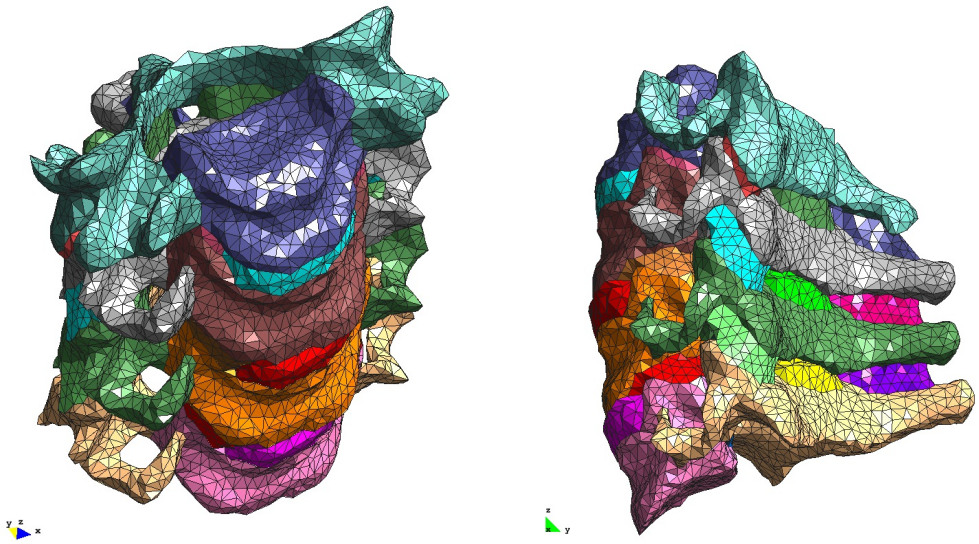

Figure 2: C3-C6 mesh with close to 68000 tetrahedral solid elements. Anterior view (left) and side view (right).

where $\mathbf{S}$ is the 2^{nd} Piola-Kirchhoff stress and $\mathbf{E}$, its conjugate, the rate of Green-Lagrange strain. Thus, stress is obtained from a scalar strain energy function or elastic potential, Ψ, and can be expressed in terms of the right Cauchy-Green deformation tensor, $\mathbf{C}$, as

$$\mathbf{S} = 2\frac{\partial \Psi\left(\mathbf{C}\right)}{\partial \mathbf{C}} \tag{2}$$

The isotropic compressible neo-Hookean hyperelastic model in reference configuration proposed by Bonet and Wood (2008) has been used. Its main advantadge, in addition to its straightforward implementation, is that the model can be characterized with the familiar material parameters used in linear elastic analyses, namely, the Young's modulus (E) and the Poisson's coefficient (ν). The strain energy function is defined as

$$\Psi = \frac{\mu}{2}\left(I_{\mathbf{C}} - 3\right) - \mu \ln J + \frac{\lambda}{2}\left(\ln J\right)^2 \tag{3}$$

where λ and μ are the Lamé parameters, J is the determinant of the deformation gradient and $I_{\mathbf{C}}$ is the first invariant of $\mathbf{C}$. Then, the constitutive equation obtained is

$$\mathbf{S} = \mu\left(\mathbf{I} - \mathbf{C}^{-1}\right) + \lambda\left(\ln J\right)\mathbf{C}^{-1} \tag{4}$$

The numerical algorithm followed is outlined in Fig. 6.

2.2.2 Scalar Damage

The isotropic damage model is based on the concept of effective stress first introduced by Kachanov (1999). The effective stress, $\bar{\mathbf{S}}$, interprets the change in mechanical behaviour of a damaged material as a loss of effective area. Thus, a damage variable is used to characterize the state of damage, which transforms the homogenized stress tensor, $\mathbf{S}$, into the effective stress tensor, $\bar{\mathbf{S}}$. For the scalar model, this variable is the scalar damage parameter d , which is directly a measure of the loss of rigidity in the material and must be within the limits $d \in [0, 1]$. A value of $d = 0$ represents an undamaged material state

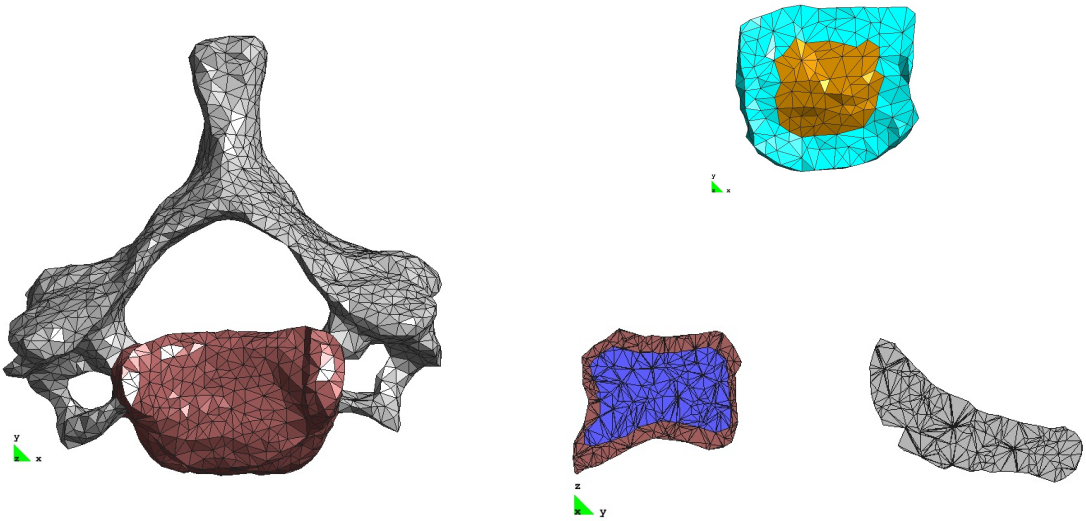

Figure 3: Top view of the C4 vertebra (left), C3-C4 intervertebral disc (top right) and vertical cut of the C4 vertebra among the z-y plane (bottom right).

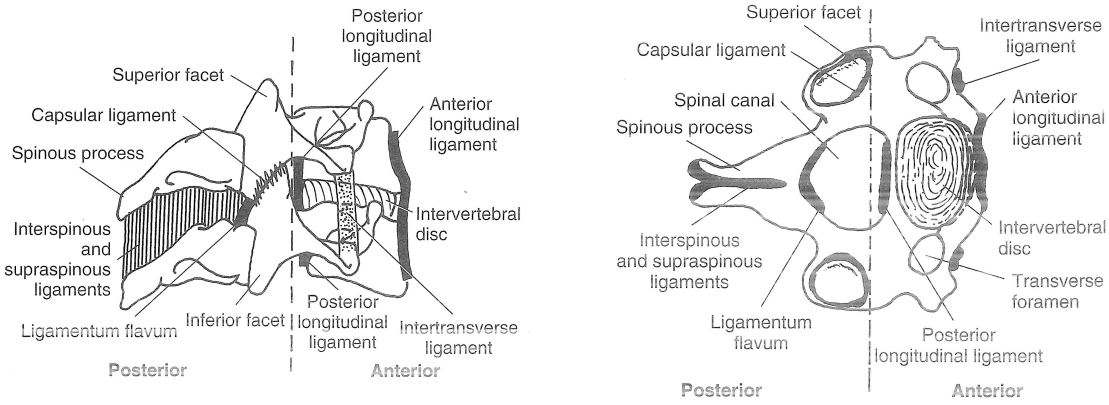

Figure 4: Schematic illustration of the ligamentous structures in the middle and lower cervical spine, extracted from Nordin and Frankel (2001). Lateral view (left) and top view (right).

whilst $d = 1$ represents a material state such that the material is completely degraded. This state can represent anything ranging from initial (macro)crack formation to local rupture, depending on what one defines as full material damage:

$$\bar{\mathbf{S}} := \frac{\mathbf{S}}{(1-d)} \tag{5}$$

Postulating the existence of a thermodynamic potential, the Helmholtz free energy $\Psi = \Psi(\mathbf{E}, \theta, d)$, and assuming the continuous medium is isothermal $\left(\dot{\theta} = 0\right)$ and has a uniform temperature distribution $(\nabla\theta = 0)$, the Clausius-Duhem inequality is reduced to

$$\mathbf{S} = \frac{\partial \Psi}{\partial \mathbf{E}} \tag{6}$$

The Helmholtz free energy is defined as

$$\begin{aligned} \Psi = \Psi(\mathbf{E}, d) &= (1-d) \cdot \Psi_0(\mathbf{E}) \\ \Psi_0(\mathbf{E}) &= \tfrac{1}{2}\mathbf{E} : \mathbb{C}^0 : \mathbf{E} \end{aligned} \tag{7}$$

Tissue	Young's Modulus (MPa)	Poisson's Ratio (-)	Initial Damage Threshold (MPa)	Tensile Fracture Energy ($Pa \cdot m^2$)
Cortical bone	10 000	0.3	200	$257.5 \cdot 10^3$
Trabecular bone	450	0.25	3.5	4.125
Posterior bone	3500	0.22	40	$71.5 \cdot 10^3$
Disc annulus	3.4	0.4	–	–
Disc nucleus	3.4	0.49	–	–
Posterior longitudinal ligament	12.5	0.39	–	–
Ligamentum flavum	2.4	0.39	–	–
Interspinous ligament	3.4	0.39	–	–
Uncovertebral joint	10^8	0.01	–	–
Zygapophyseal joint	10^8	0.01	–	–

Table 1: Material properties of the tissues used in the finite element model of the cervical spine.

where $\Psi_0(\mathbf{E})$ is the Helmholtz free energy of the undamaged material in its initial state and $\mathbb{C}_0$ is the corresponding elastic constitutive tensor.

Then, the constitutive equation obtained is

$$\mathbf{S} = \frac{\partial \Psi}{\partial \mathbf{E}} = (1-d)\,\frac{\partial \Psi_0}{\partial \mathbf{E}} = (1-d)\,\mathbb{C}^0 : \mathbf{E} \tag{8}$$

This damage model is characterized by:

- The model's formulation is similar to that derived under infinitesimal strain theory, but is integrated in the Total Lagrangian framework, that is, the Green-Lagrange strain tensor is used to formulate the constitutive equation. Note that the FE problem has been solved in the reference configuration using large deformation theory because the hyperelasticity model requires it. However, it has been considered that the bone tissues, which are the materials using the damage model, do not suffer large strains and, thus this damage model suffices.

- There exists a threshold that differentiates the elastic state from the damaged one and is defined in an analogous way to the yield criterion in plasticity models,

$$\mathbb{F}\left(\bar{\mathbf{S}}, d\right) = f\left(\bar{\mathbf{S}}\right) - c\,(d) \leq 0 \tag{9}$$

  where $f\left(\bar{\mathbf{S}}\right)$ is a scalar function of the effective stress tensor and $c\,(d)$ is a scalar function that defines the position of the damage threshold. The initial value of the damage threshold, $c\,(d^0) = \mathbf{S}_0^d$, is a material property. Here $f\left(\bar{\mathbf{S}}\right)$ follows the Mohr-Coulomb criteria with the parameters shown in Table 2.

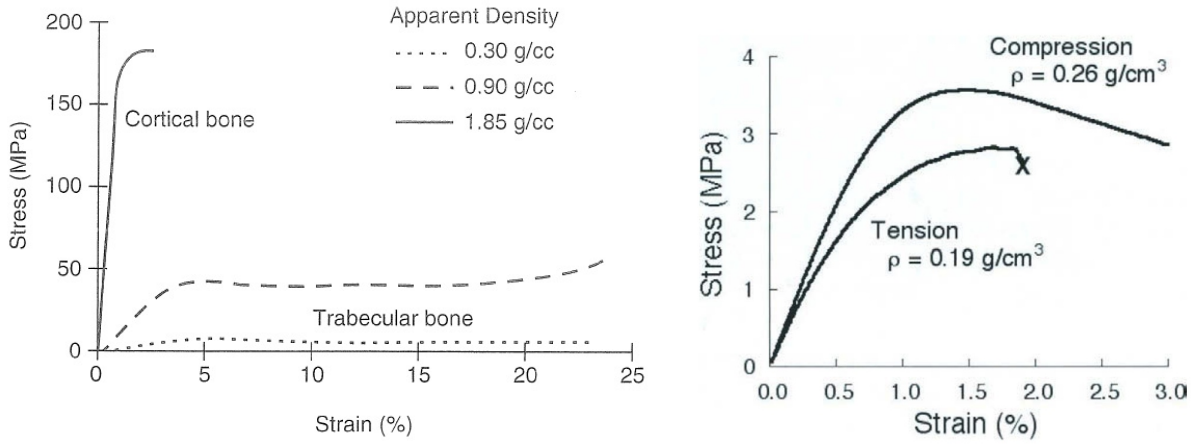

Figure 5: Stress-strain curve of cortical and trabecular bone in compression from Nordin and Frankel (2001) (left) and of trabecular bone in tension and compression from Kurtz and Edidin (2006) (right).

- The integration of the constitutive equation is explicit and the evolution of the internal damage variable is assumed to be linear through the scalar function

$$d = \frac{1 - \dfrac{\mathbf{S}_0^d}{f\left(\bar{\mathbf{S}}\right)}}{1 + H} \tag{10}$$

where $\mathbf{S}_0^d$ is the material property initial damage threshold, whose magnitude is in the compression scale and must have a value such that $0 \leq \mathbf{S}_0^d \leq f\left(\bar{\mathbf{S}}\right)$, and H is a parameter defined as:

$$H = \frac{-\left(\mathbf{S}_0^d\right)^2}{2E \cdot g_f^d \cdot \left(R_0^d\right)^2} \tag{11}$$

Where

  - E is the Young's Modulus of the material.
  - g_f^d is the maximum fracture energy dissipated at each point, calculated as $g_f^d = {}^{G_f^d}/_h$ where G_f^d is the tensile fracture energy of the material and h is the fracture length of the element.
  - R_0^d is the relation between initial stresses existing between the tensile and compressive limits, $R_0^d = |\mathbf{s}_0^C/\mathbf{s}_0^T|$.

Parameter	Value
ψ_{max}	15°
φ_{max}	15°
$R_0 = \left\lvert \frac{\mathbf{S}_0^{dC}}{\mathbf{S}_0^{dT}} \right\rvert$	1.4
G_c	$= G_f \cdot R_0^2$

Table 2: Additional parameters used in the definition of the damage model for the bone tissues in the finite element model of the cervical spine.

Initial data for the current Gauss Point:

- Deformation gradient, $\mathbf{F}$
- Determinant of the deformation gradient, J.

Material properties:

- Reading of E and ν for the given material and calculation of λ and μ.

Verification of the formulation used:

Total Lagrangian

- Calculate the right Green-Cauchy tensor: $\mathbf{C} = \mathbf{F}^T \cdot \mathbf{F}$.
- Calculate its inverse tensor, $\mathbf{C}^{-1}$.
- Calculate the 2^{nd} Piola Kirchhoff stress,

$$\mathbf{S} = \mu \left(\mathbf{I} - \mathbf{C}^{-1}\right) + \lambda \left(\ln J\right) \mathbf{C}^{-1}$$

- Calculate the material elasticity tensor,

$$\mathbb{C}^{tan} = \lambda \mathbf{C}^{-1} \otimes \mathbf{C}^{-1} + 2\left(\mu - \lambda \ln J\right) \mathcal{I}$$

Store calculated stress and tangent constitutive tensors.

Figure 6: Numerical integration (at each load increment) of the neo-Hookean constitutive equation used to model the ligament and disc tissues.

- All the components of the stress tensor are equally damaged so the Poisson's ratio of the material remains constant.
- The numerical algorithm followed is outlined in Fig. 7.

2.3 Boundary Conditions and Loadings

An initial load case was carried out where the load of the head was simulated by imposing an axial load of 60N (Yoganandan et al. (2009); Li and Lewis (2010)) distributed among the nodes of the top surface of the top vertebra's body. The nodes of the bottom surface of the bottom vertebra's body were totally restricted. A contraction of the ligaments was imposed in order to account for the initial pre-stressed state of ligaments in a healthy vertebral column. This contraction has been induced as a thermal contraction by defining a fictitious volumetric thermal expansion coefficient, α, and temperature increment, $\Delta\theta$, such that the thermal strain, ϵ^t, is obtained from Eq. (12). Table 3 shows the contraction values considered for each ligament.

$$\epsilon^t = \alpha \, \Delta\theta \, \mathbf{1} \tag{12}$$

Then, the results were subjected to the following loadings: (1) a flexion moment of $1N{\cdot}m$, (2) an extension moment of $1N{\cdot}m$, (3) a right lateral bending of $1N{\cdot}m$ and (4) a left lateral bending of $1N{\cdot}m$. These were compared with previously published results by Kallemeyn et al. (2010) to ensure the FE model exhibited an adequate behaviour.

Initialization of variables for the current Gauss point:

- Damage variable, $d^0 = d^{ant} = 0$.
- Accumulated damage in the structure in the previous iteration, $\mathrm{D}^{ant} = 0$.
- Dissipation due to the current increment, $\gamma = 0$.
- Accumulated dissipation in the structure in the previous iteration, $\Xi^{ant} = 0$.
- Initial value of the position of the damage threshold, $c\left(d^0\right) = \mathbf{S}_0^d$.

→ Load step increment:

- Calculation of the predictor elastic stress, $\bar{\mathbf{S}} = \mathbb{C}^0 : \mathbf{E}$.
- Calculation of the scalar function of the stress tensor, $f\left(\bar{\mathbf{S}}\right)$, according to the chosen criterion (Mohr-Coulomb).

Verification of the damage threshold criterion:

$f\left(\bar{\mathbf{S}}\right) < c\left(d\right)$?

→ **NO** → **DAMAGED MATERIAL:**

- Update of the damage threshold, $c\left(d\right) = f\left(\bar{\mathbf{S}}\right)$
- Calculation of the damage variable, d:

  Linear softening

  $$d = \frac{1-\frac{\mathbf{S}_0^d}{f(\bar{\mathbf{S}})}}{1+H} \text{ with } H = \frac{-\left(\mathbf{S}_0^d\right)^2}{2E_0 g_f^d \left(R_0^d\right)^2}$$

- Calculation of the dissipation generated in this load increment, $\gamma = \triangle d \cdot \Psi_0$ where the damage variable increment is $\triangle d = d - d^{ant}$.
- Actualization of the variable d^{ant}: $d^{ant} = d$.
- Calculation of the tangent constitutive tensor,

  $$\mathbb{C}^T = \left(1-d\right)\mathbb{C}^0 - \frac{\partial G\left[f(\bar{\mathbf{S}})\right]}{\partial f(\bar{\mathbf{S}})}\bar{\mathbf{S}} \otimes \left[\frac{\partial f(\bar{\mathbf{S}})}{\partial \mathbf{E}}\right]$$

- Go to $*$.

→ **YES** → **ELASTIC MATERIAL:**

- No action is taken. Continue to $*$.

$*$ Actualization of:

- the stress state, $\mathbf{S} = \left(1-d\right)\bar{\mathbf{S}}$.
- the accumulated dissipation in the structure, $\Xi = \Xi^{ant} + \gamma \cdot \mathrm{V}$.
- the accumulated damage in the structure, $\mathrm{D} = \mathrm{D}^{ant} + d \cdot \mathrm{V}$.

(V is the volume of the Gauss point being integrated.)

Figure 7: Numerical integration of the explicit damage constitutive equation used to model the bone tissue.

Ligament	α ($^1/_{^\circ C}$)	$\Delta\theta$ ($^\circ$C)
Posterior longitudinal ligament	$2 \cdot 10^{-3}$	-25
Ligamentum flavum	$2 \cdot 10^{-6}$	-25
Interspinous ligament	$2 \cdot 10^{-6}$	-25

Table 3: Contraction parameters used in the different ligaments in the finite element model of the cervical spine.

Finally, the load case corresponding to the distraction applied by the forceps in a discectomy operation was simulated by pulling apart the C4 and C5 vertebrae (Fig. 8 (left)). This load case was applied on the outcome of the initial head load case. The nodes where the head load was applied in the previous load case were now completely fixed at their present position. A displacement was then forced on the group of nodes at the base of the arrows shown in Fig. 8 (right). This displacement is forced in the direction (upwards or downwards) indicated by the arrows.

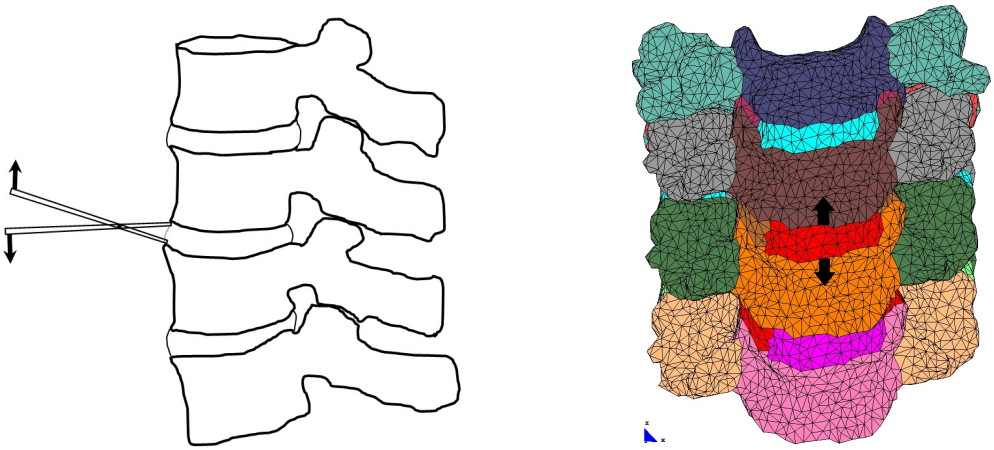

Figure 8: Scheme of the imposed loads on the vertebral bodies in an ACD (left) and forced displacement on the FE model simulating these loads (right).

3 RESULTS

The results for the flexo-extension and the lateral bending loading cases are compared with the results obtained by Kallemeyn et al. (2010) in Fig. 9. Note that Kallemeyn's results correspond to their baseline C2-C7 model which "has provided reasonable results for models previously compared to experimental data in literature". It can be seen that the flexo-extension curve obtained is closer to Kallemeyn's in flexion than in extension. This is most probably due to the fact that the anterior longitudinal ligament was not included in the model. Similarly, the lateral bending curve shows less agreement with the reference curve than the flexo-extension one because the intertransverse ligament, not modelled in the FE spine, may have an appreciable contribution in this type of movement. Finally, the results obtained behave in a more linear manner than the reference ones, possibly because the hyperelastic model chosen for the ligaments is not sufficiently non-linear. Also, the anatomically inaccurate geometry of the C5 and C6 vertebrae, as well as the fact that the C2 and C7 vertebrae are not present in the model, might be accountable for these

differences.

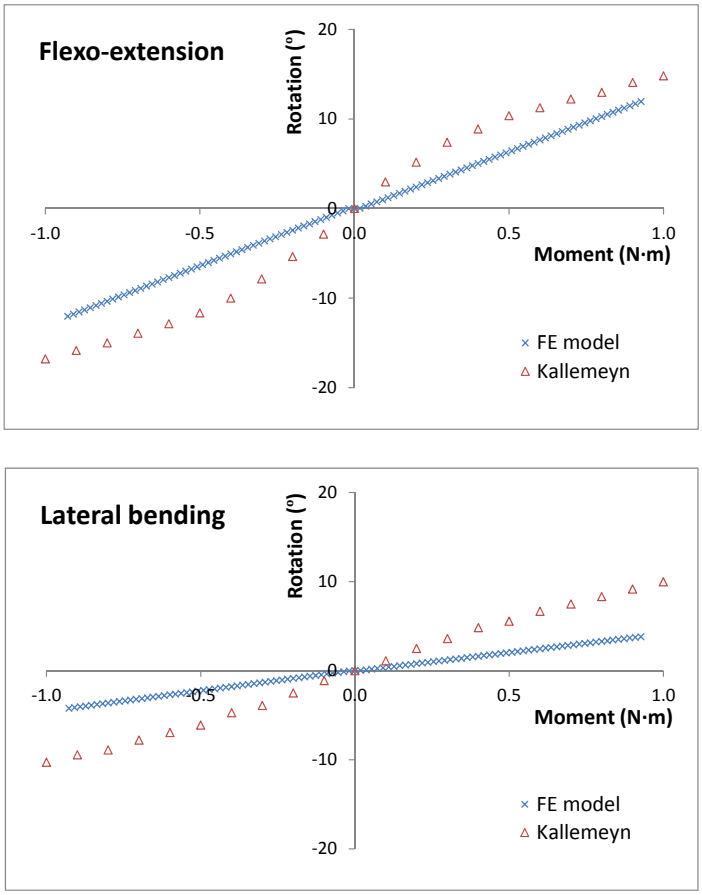

Figure 9: Flexo-extension (above) and lateral bending (below) results of the C3-C6 finite element model.

The displacement results of the model's mid vertical plane due to the discectomy loading case are shown in Fig. 10. The maximum displacement corresponds to a value of $0.23mm$, which is the value reached in the last step of forced displacement on the C4 and C5 vertebrae. This loading induces damage mostly in the trabecular bone adjacent to the loading spots, as shown in Fig. 11. However, all vertebrae suffer varying degrees of stresses, being the highest concentrations around the uncovertebral joints (see Fig. 12). The adjacent intervertebral discs suffer much lower stresses, as observed in Fig. 13.

4 CONCLUSIONS

The three-dimensional (3D) finite element (FE) analysis of an anterior cervical discectomy (ACD) presented in this study offers an insight into understanding the internal mechanical response of the spine to the loads induced by the surgical procedure, which may lead to improved techniques during this procedure. In addition, the use of digitalized quantitative axial computed tomography (CT) scans to obtain geometrically accurate FE models offers the possibility of using specimen-specific models which might allow to tailor each surgical procedure to the needs and particular situation of each patient. However, to this end, the model proposed in the present study undoubtedly needs to be refined.

Figure 10: Displacements (x30) of the mid vertical plane due to the forced displacement imposed on the C3-C6 FE model to simulate the discectomy operation.

The C3-C6 spine model developed comprises the vertebral bodies (divided into the posterior part, the body's cortical shell and the body's trabecular core), the intervertebral discs (with the annulus and nucleus distinguished), the uncovertebral and zygapophyseal joints and the main ligaments (PLL, LF and IL). An isotropic scalar damage model was used for the bone tissue whilst the discs and ligaments were assigned an isotropic neo-Hookean hyperelastic material.

First, the model was subjected to a flexion-extension and a lateral bending loadings in order to assess the validity of the model by comparison with previously published results by Kallemeyn et al. (2010). These loadings were imposed on the model after prestressing the ligaments and applying an axial head load of 60N. No meaningful quantitative comparison can be made between the results obtained in the present study and the ones by Kallemeyn because their model comprises nearly the full cervical spine (C2-C7). Nevertheless, interesting judgments can be derived in the wake of this validation load case. The most obvious of these judgments is that the model is lacking in non-linear response as seen in Fig. (9). This can be attributed to, on the one hand, an inadequate hyperelastic model, and, on the other hand, an incomplete modelling of the ligaments. As to the former reason, neo-Hookean hyperelasticity was chosen because it is characterized by the material parameters used in linear elastic analyses (Young's modulus and Poisson's ratio), without requiring any additional parameters. Considering that the great majority of literature available where FE cervical spine models are developed work solely with linear elastic materials, this seemed an appropriate choice. In retrospect, a more elaborate hyperelastic model might be needed to capture the highly non-linear behaviour of ligamentous tissue in detriment of simplicity in parameters. With respect to the latter reason, the excluded ligaments, especially the anterior longitudinal ligament (ALL) and the intertransverse ligament (ItL), were not believed to contribute significantly in the ACD procedure and, thus, where not modelled. One must note that, unlike most other authors, in the present study ligaments were modeled in detail in 3D with the same tetrahedral elements as the

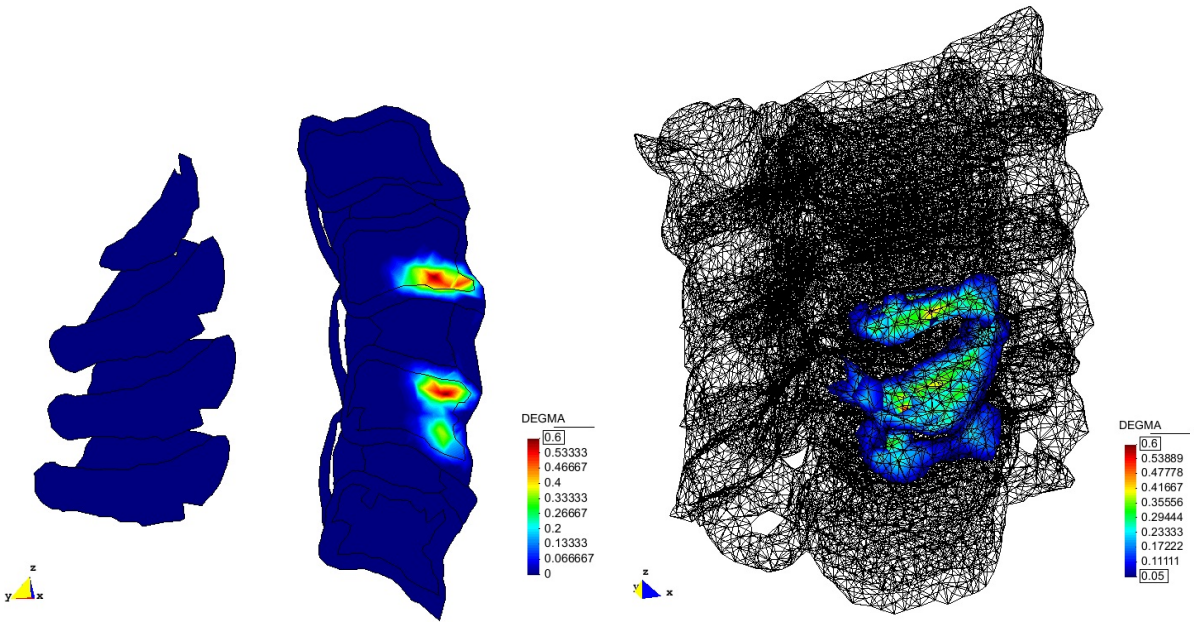

Figure 11: Damage in the mid vertical plane (left) and in the whole model (right) due to the forced displacement imposed on the C3-C6 FE model to simulate the discectomy operation. Displacements x20.

rest of the model. Yet, the missing ligaments might be key to achieving quantitatively accurate results in the flexo-extension and lateral bending loadings. Lastly, it is worth mentioning that the validation load case has been performed in such a way that only one reference is available for comparison. Most authors choose to perform these validation cases in spine units of two adjacent vertebrae and their corresponding intervertebral disc and ligaments. Therefore, in order to achieve a precise validation of the model, it would be interesting to perform these set of additional simulations.

Finally, the ACD load case was performed by pulling apart the C4 and C5 vertebrae. Again, these loads were applied on the outcome of the initial head load case. The results obtained are promising as they seem coherent with the forced displacements imposed. However, if the ACD simualtion is to lead to a well-founded understanding of the internal mechanical response of the spine to the induced loads, it is essential that the limitations of this model be overcome so that the results are *qualitatively* and *quantitatively* adequate. First and foremost, the C5 and C6 vertebrae models, which were obtained by copying the C4 vertebra model, should be replaced by models obtained from actual CT scans of these vertebrae. Including the C2 and C7 vertebrae would be commonsense for the sake of completness. Next, the ligaments could be modelled more accurately, as mentioned above. In addition to the aspects previously discussed, the geometry of certain ligaments, in particular, the PLL, could be improved with the aid of adequate anatomical references. Also, the prestress values imposed on the ligaments should be better calibrated. Unfortunately, it has proven impossible for the authors to obtain literature with exact prestress values of these tissues. Nonetheless, a more sophisticated hyperelastic model together with the literature available on stress-strain behaviour of the different ligaments (for example, Ivancic et al. (2007)) might allow to accomplish this without need of exact prestress values. Furthermore, the validity of using a damage formulation in a large deformation framework which is derived in a similar way to a damage formulation in an infinitesimal

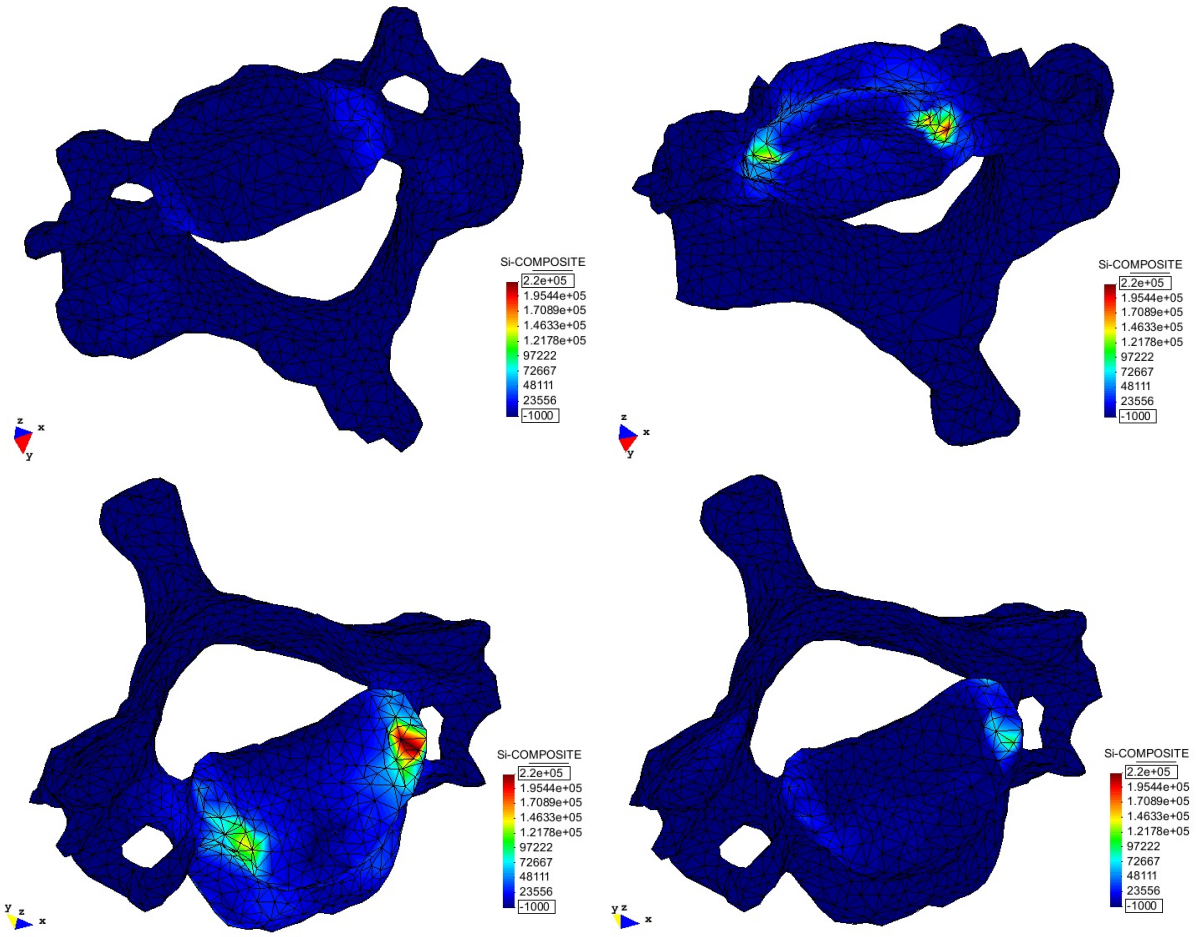

Figure 12: Stresses in the C3 (above left), C4 (above right), C5 (below left) and C6 (below right) vertebrae due to the forced displacement imposed on the C3-C6 FE model to simulate the discectomy operation. Displacements x20. Values given in 10^3Pa.

strain framework should be studied in more detail. Finally, the results obtained with the proposed refinements could be further improved by introducing anisotropy into the model, especially in the ligaments and intervertebral discs. The use of composite materials to represent the fibers in the disc annulus could also be considered. Another aspect to take into account is the actual ACD procedure and how this has been numerically modelled. Other tools, in addition to the one used to separate the vertebrae appart, are used (such as tools to keep the displaced vertebrae in place) and these might induce loads which have not been considered here.

To sum up, even though the FE analysis of the ACD procedure presented in this study yields qualitatively acceptable results, the model requires some refinement in order to achieve its proposed ultimate goal, which is to aid the neurosurgeons performing this procedure to better understand the biomechanics of how the spine internally responds to the imposed loads during the surgery.

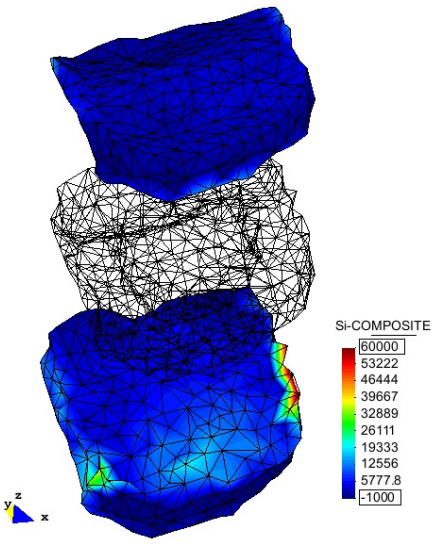

Figure 13: Stresses in the C3-C4 and C5-C6 intervertebral discs due to the forced displacement imposed on the C3-C6 FE model to simulate the discectomy operation. Displacements x20.

REFERENCES

Bonet J. and Wood R.D. *Nonlinear Continuum Mechanics for Finite Element Analysis*. Cambridge University Press, Cambridge, 2 edition, 2008.

del Palomar A.P., Calvo B., and Doblaré M. An accurate finite element model of the cervical spine under quasi-static loading. *Journal of Biomechanics*, 41(3):523–531, 2008.

DeWit J.A. Cervical spine segment finite element model for traumatic injury prediction. *Journal of the mechanical behavior of biomedical materials*, 10:138–150, 2012.

Donaldson J.W. and Nelson P.B. Anterior cervical discectomy without interbody fusion. *Surgical neurology*, 57(4):219–224, 2002.

Hussain M., Nassr A., Natarajan R.N., An H.S., and Andersson G.B.J. Corpectomy versus discectomy for the treatment of multilevel cervical spine pathology: a finite element model analysis. *The Spine Journal*, 12(5):401–408, 2012.

Ivancic P.C., Coe M.P., Ndu A.B., Tominaga Y., Carlson E.J., Rubin W., Dipl-Ing F.H., and Panjabi M.M. Dynamic mechanical properties of intact human cervical spine ligaments. *The Spine Journal*, 7(6):659–665, 2007.

Kachanov L.M. Rupture time under creep conditions. *International Journal of Fracture*, 97(1):11–18, 1999.

Kallemeyn N., Gandhi A., Kode S., Shivanna K., Smucker J., and Grosland N. Validation of a c2–c7 cervical spine finite element model using specimen-specific flexibility data. *Medical engineering and physics*, 32(5):482–489, 2010.

Kumaresan S., Yoganandan N., and Pintar F.A. Finite element analysis of the cervical spine: a material property sensitivity study. *Clinical Biomechanics*, 14(1):41–53, 1999.

Kurtz S.M. and Edidin A.A. *Spine technology handbook*. Elsevier Academic Press, Amsterdam; Boston, 2006.

Li Y. Association between extent of simulated degeneration of c5-c6 disc and biomechanical parameters of a model of the full cervical spine: A finite element analysis study. *Journal of Applied Biomaterial and Biomechanics*, 8(3):191–199, 2010.

Li Y. and Lewis G. Influence of surgical treatment for disc degeneration disease at c5–c6

on changes in some biomechanical parameters of the cervical spine. *Medical engineering and physics*, 32(6):595–603, 2010.

Netter F.H. *Sistema Nervioso, Anatomia y Fisiologia. Tomo 1.1.* Masson, 1999.

Nordin M. and Frankel V.H. *Basic biomechanics of the musculoskeletal system.* Lippincott Williams and Wilkins, Philadelphia etc., 3 edition, 2001.

Tchako A. Stress changes in intervertebral discs of the cervical spine due to partial discectomies and fusion. *Journal of biomechanical engineering*, 131(5), 2009.

Teo E.C. and Ng H.W. Evaluation of the role of ligaments, facets and disc nucleus in lower cervical spine under compression and sagittal moments using finite element method. *Medical engineering and physics*, 23(3):155–164, 2001.

Yoganandan N., Pintar F.A., Zhang J., and Baisden J.L. Physical properties of the human head: Mass, center of gravity and moment of inertia. *Journal of Biomechanics*, 42(9):1177–1192, 2009.

Zhang J.G. A three-dimensional finite element model of the cervical spine: An investigation of whiplash injury. *Medical biological engineering computing*, 49(2):193–201, 2011.

Zhang Q.H., Teo E.C., and Ng H.W. Development and validation of a c0-c7 fe complex for biomechanical study. *Journal of Biomechanical Engineering*, 127(5):729–735, 2005.

Zhang Q.H., Teo E.C., Ng H.W., and Lee V.S. Finite element analysis of moment-rotation relationships for human cervical spine. *Journal of Biomechanics*, 39(1):189–193, 2006.